Journal of General Virology (2003), **84**, 3291–3303 DOI 10.1099/vir.0.19505-0

Proliferative growth of SARS coronavirus in Vero E6 cells

M.-L. Ng,[1,2] S.-H. Tan,[2] E.-E. See,[3] E.-E. Ooi[3] and A.-E. Ling[4]

[1,2]Department of Microbiology[1] and Electron Microscopy Unit, Faculty of Medicine[2], 5 Science Drive 2, National University of Singapore, 117597, Singapore

[3]Environmental Health Institute, National Environment Agency, Singapore

[4]Department of Pathology, Singapore General Hospital, Singapore

Correspondence
Mah-Lee Ng
(at Department of Microbiology)
micngml@nus.edu.sg

Received 14 July 2003
Accepted 19 August 2003

An isolate of SARS coronavirus (strain 2003VA2774) was obtained from a patient and used to infect Vero E6 cells. The replication cycle of the virus was followed from 1 to 30 h post-infection (p.i.). It was surprising to observe the swift growth of this human virus in Vero cells. Within the first hour of infection, the most obvious ultrastructural change was the proliferation of the Golgi complexes and related vesicles accompanied by swelling of some of the *trans*-Golgi sacs. Extracellular virus particles were present by 5 h p.i. in about 5 % of the cells and this increased dramatically to about 30 % of the cell population within an hour (6 h p.i.). Swollen Golgi sacs contained virus nucleocapsids at different stages of maturation. These virus precursors were also in large vacuoles and in close association with membrane whorls. The membrane whorls could be the replication complexes, since they appeared rather early in the replication cycle. As infection progressed from 12 to 21 h p.i., the cytoplasm of the infected cells was filled with numerous large, smooth-membraned vacuoles containing a mixture of mature virus and spherical cores. Several of these vacuoles were close to the cell periphery, ready to export out the mature progeny virus particles via exocytosis. By 24 to 30 h p.i., crystalline arrays of the extracellular virus particles were seen commonly at the cell surface.

INTRODUCTION

SARS CoV (severe acute respiratory syndrome coronavirus) is a new virus that was identified during the recent SARS outbreak, which started in southern China and spread to Hong Kong, Vietnam, Canada and Singapore. SARS CoV was isolated using Vero E6 cells (Drosten *et al.*, 2003; Ksiazek *et al.*, 2003). Sequence analyses of various isolates have indicated that although this virus shares many similarities with coronaviruses, it is genetically distinct to all known coronaviruses (Marra *et al.*, 2003; Rota *et al.*, 2003; Ruan *et al.*, 2003).

The family *Coronaviridae* is made up of a collection of viruses that cause prevalent diseases in humans and domestic animals (Holmes, 1990). The known human coronaviruses (HCoV-229E and HCoV-OC43) often cause cold-like symptoms that contrast with the recent infections caused by SARS CoV.

In general, the latent periods of coronaviruses can be relatively short in tissue culture (about 6 h) (Sturman & Takemoto, 1972). Infection can be cytocidal for the cells or, in some cases, persistent infection can result depending on the virus strain and cell type (Wege *et al.*, 1982; Sturman & Holmes, 1983; Frana *et al.*, 1985). Cell cultures infected with HCoV-229E were able to produce virus particles over weeks without any expression of cytopathic effects (Chaloner-Larsson & Johnson-Lussenburg, 1981), as only a portion of the cells are infected (Lucas *et al.*, 1978; Holmes & Behnke, 1981; Lamontagne & Dupuy, 1984).

Coronaviruses have strong tissue tropism and will often grow in cells of the natural host species (Fleming *et al.*, 1987, 1988; Sussman *et al.*, 1987). The site of replication is in the cytoplasm of the infected cells (Wilhelmsen *et al.*, 1981). The virus assembles by budding at the Golgi complex (David-Ferreira & Manaker, 1965; Tooze *et al.*, 1984; Tooze & Tooze, 1985). The maturation site appears to be determined by the presence of one of the virus envelope glycoproteins, E1 (Sturman *et al.*, 1980; Holmes *et al.*, 1981a, b, 1984; Sturman & Holmes, 1983). The virus particles migrate through the Golgi complex where glycosylation and processing of the envelope glycoproteins take place. The mature virus particles are then transported in smooth-walled vacuoles to the cell periphery (Sturman & Holmes, 1983; Holmes *et al.*, 1984).

Fusion occurs between the vacuolar walls and the plasma membrane to extrude the progeny virus particles. Extracellular virus particles are usually seen to accumulate in large quantities along the plasma membranes of the infected cells (Oshiro, 1973).


a
Nu
M
M
0.5 μm

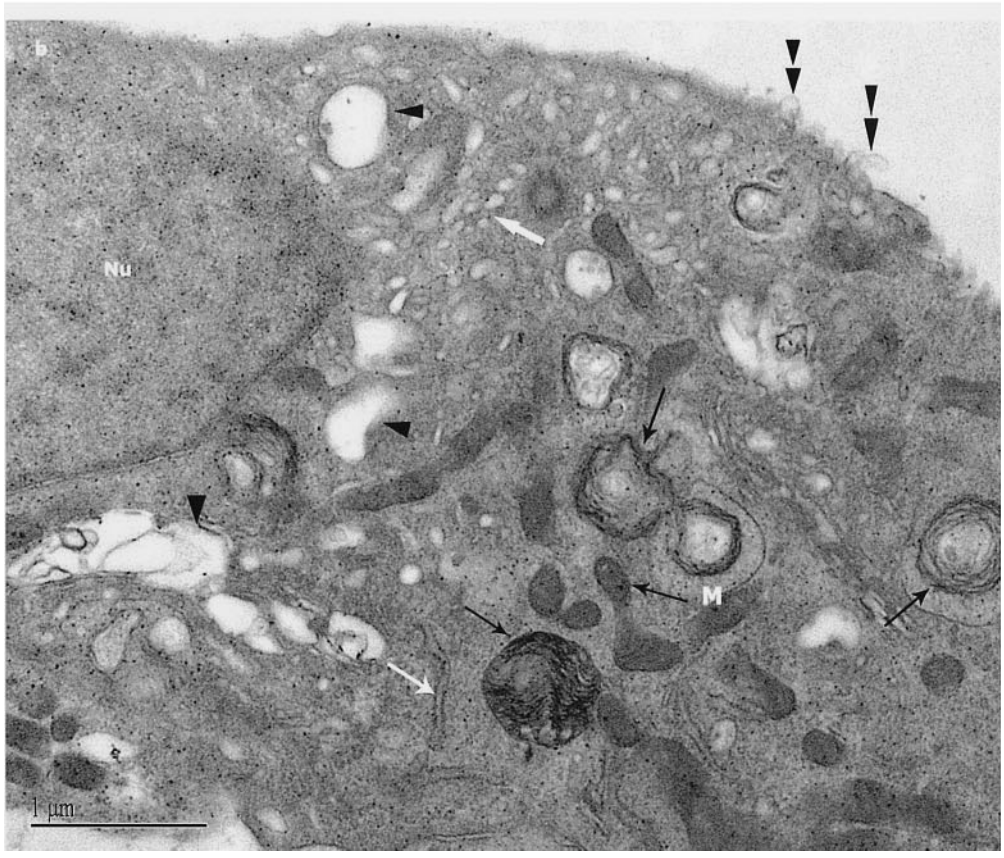
b
Nu
M
1 μm

Unlike the known human coronaviruses, SARS CoV infections often result in severe disease. This electron microscopic study aims to determine if there are any unique features during the SARS CoV replication process that can be related to the severity of the disease seen during this outbreak.

METHODS

Cells and virus. SARS CoV (strain 2003VA2774) was isolated from a SARS patient in Singapore by the Department of Pathology, Singapore General Hospital. The virus was subsequently grown in Vero E6 cells (ATCC #C1008) for 24 h in the Environmental Health Institute, Singapore. The titre of this virus stock was 1×10^7 p.f.u. ml^{-1} and was used to infect new cell monolayers for this study.

Electron microscopy. The replication cycle of SARS CoV was followed at hourly intervals between 1 and 6 h post-infection (p.i.) and subsequently at intervals of 6 h until 30 h p.i. At the appropriate time, cells were fixed with 5 % glutaraldehyde and 2·5 % paraformaldehyde for 4 h. Following the fixation period, the infected monolayer was washed with cold PBS before fixation with 1 % osmium tetroxide. The cells were then dehydrated with a series of ethanol of ascending percentages and embedded in low-viscosity epoxy resin. The cells in resin were polymerized before ultramicrotomy was performed. Ultrathin sections were stained with 2 % uranyl acetate and post-fixed with 2 % lead citrate before viewing under the electron microscope (CM 120 BioTwin, Philips). Images were captured digitally with a Dual View digital camera (Gatan). Ultrastructural studies were performed in the Electron Microscopy Unit, Faculty of Medicine, National University of Singapore.

RESULTS

Vero E6 cells were infected with SARS CoV, isolated during the recent outbreak in Singapore. A time sequence study was conducted from 1 to 30 h p.i.

In a previous study by Ng *et al.* (2003), it was observed that SARS CoV was internalized and uncoated within 30 min of infection. In addition, there was smooth membrane induction within the smooth-membraned vacuoles containing these nucleocapsids.

In mock-infected cells, the morphology of the various cell organelles was normal (Fig. 1a). During the first hour after infection with SARS CoV (Fig. 1b), however, there were already several vacuoles containing membrane whorls (Fig. 1b, arrows). The other obvious ultrastructural change was the swelling of the Golgi sacs at the perinuclear region (Fig. 1b, arrowheads) and proliferation of the *trans*-Golgi vesicles (thick white arrow). However, the rough endoplasmic reticulum (Fig. 1b, thin white arrow) remained normal in morphology. Fused virus envelopes at the plasma membrane similar to that of the 20–30 min p.i. cells were seen also (Fig. 1b, double arrowheads) (Ng *et al.*, 2003).

By 3 h p.i., precursor viruses (50 nm) (Fig. 2a, arrows) were observed in the vicinity of the swollen *trans*-Golgi complex (arrowhead). The eclipse phase for SARS CoV was found to be only 4 h p.i. (Fig. 2b). A mixture of mature progeny virus particles (100 nm) (Fig. 2b, arrows) and nucleocapsids (50nm) (white arrows) was present in the swollen sacs by this time. Extracellular progeny virus particles (Fig. 2c, arrow) were first observed at 5 h p.i. in about 5 % of the cell population, indicating the end of the latent period. The presence of large vacuoles containing virus precursors and membrane whorls (Fig. 2c, arrowheads) was found consistently in the SARS CoV-infected cells. These membrane whorls, which could be the replication complexes where viral RNA synthesis occurs, were seen early in the replication process in close association with the newly internalized nucleocapsids. The morphology of the rough endoplasmic reticulum remained unaffected by the infection (Fig. 2c, white arrows).

SARS CoV grew rapidly in Vero E6 cells and a titre of 10^7 p.f.u. ml^{-1} was obtained easily. Nonetheless, it was still surprising to observe that SARS CoV infection was well advanced by 6 h p.i. Mature extracellular virus particles were present in about 25–30 % of the cell population (Fig. 3a, arrowheads). This was a dramatic increase in the number of productive cells compared to that seen at 5 h p.i. (5 %), indicating a very rapid assembly process after the latent period. The common sight of swollen *trans*-Golgi sacs filled with membrane whorls (Fig. 3a, arrows) occupied a large area of the infected cytoplasm.

Some cells had spherical SARS CoV cores in the swollen Golgi sacs (Fig. 3b, arrowheads). Spherical cores were also found in the lumen of morphologically normal Golgi sacs (Fig. 3b, inset) and maturing virus particles appeared to be pinching off at the end of the Golgi sacs (Fig. 3b, inset, arrow). A few singly packed virus particles in small vesicles (Fig. 3b, white arrows) were very close to the cell periphery. These are most likely the transport vehicle for the progeny virus particles to the exterior.

The large vacuoles were most likely the very swollen *trans*-Golgi sacs (Fig. 4a, arrowheads). Doughnut-shaped and

Fig. 1. (a) Mock-infected Vero cells. The mock-infected cell has normal Golgi complex (arrowhead), smooth endoplasmic reticulum (arrow) and mitochondrion (M) morphology. There are no vacuoles present enclosing the membrane whorls seen in the infected cells. (b) SARS CoV-infected Vero cells at 1–2 h p.i. Obvious swollen Golgi sacs (arrowheads) are seen around the perinuclear region of the infected cells (1 h p.i.). Proliferation of the *trans*-Golgi vesicles (white thick arrow) is another change observed in the infected cells but the rough endoplasmic reticulum remains normal in morphology (white thin arrow). There are also many smooth membrane vacuoles that have many membrane whorls (arrows). The mitochondria (M) are normal in morphology. Empty envelopes from internalized nucleocapsids are fused with the infected cell plasma membrane (double arrowheads) are shown. Nu, Nucleus.

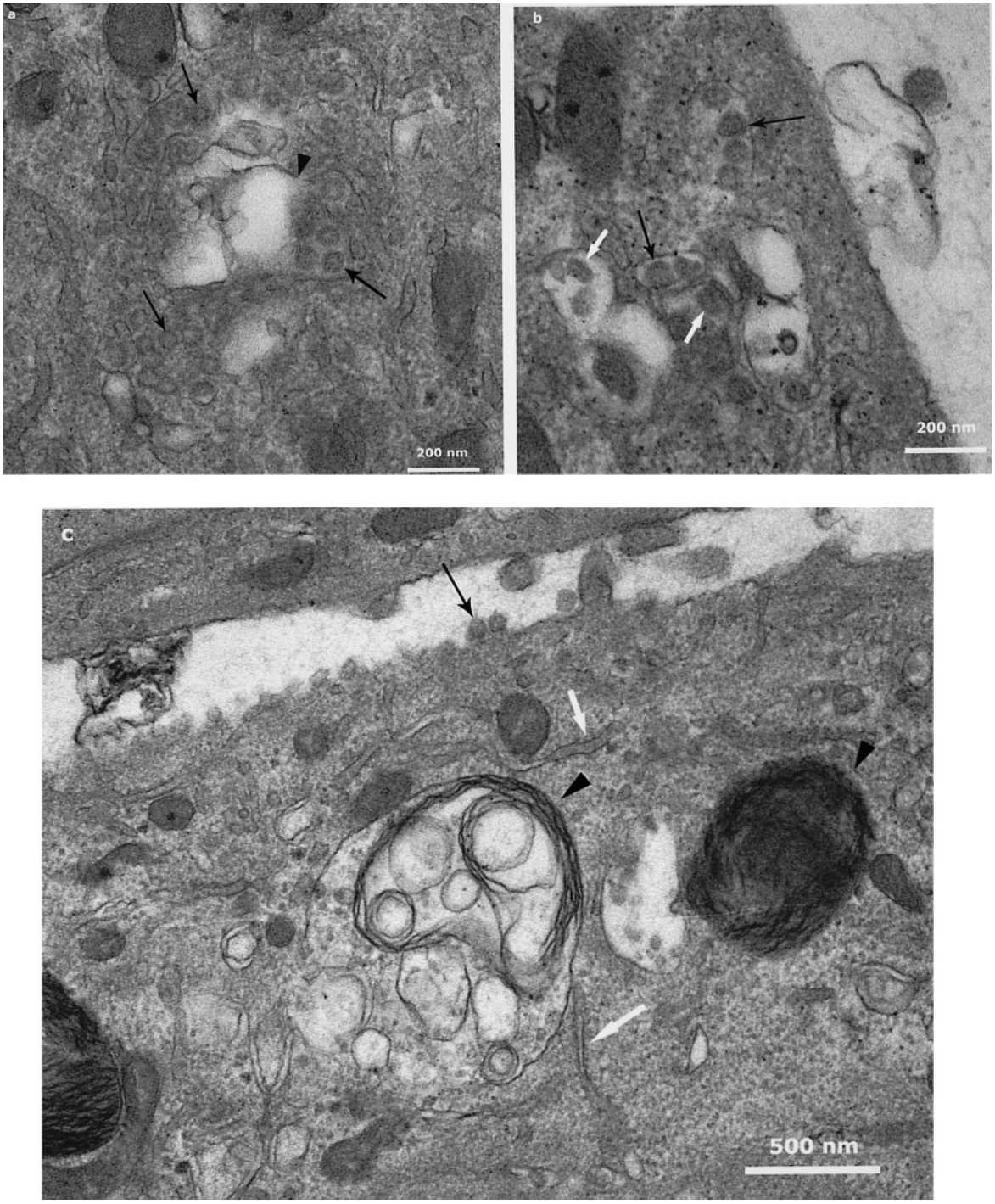

Fig. 2. SARS CoV-infected Vero cells at 3–5 h p.i. (a) At 3 h p.i., newly synthesized virus precursors (arrows) are in close vicinity of the swollen Golgi sacs (arrowhead). (b) The eclipse phase of SARS CoV infection ended at 4 h p.i. Mature progeny virus particles (arrows) are seen intermingled with the nucleocapsids (white arrows) in the swollen Golgi sacs. (c) After 5 h p.i., the first sign of extracellular virus (arrow) is seen in about 5 % of the cell population. The rough endoplasmic reticulum (white arrows) remains normal in morphology. The large smooth vacuoles with nucleocapsids and membrane whorls (arrowheads) are consistent features in the infected cells.

spherical nucleocapsids (50 nm) were found in these vacuoles. Membrane layers (Fig. 4a, arrows) associated closely with the virus cores was found in all infected cells. Mature extracellular virus particles with visible spikes on the envelopes were on the cell surface (Fig. 4a, white arrows).

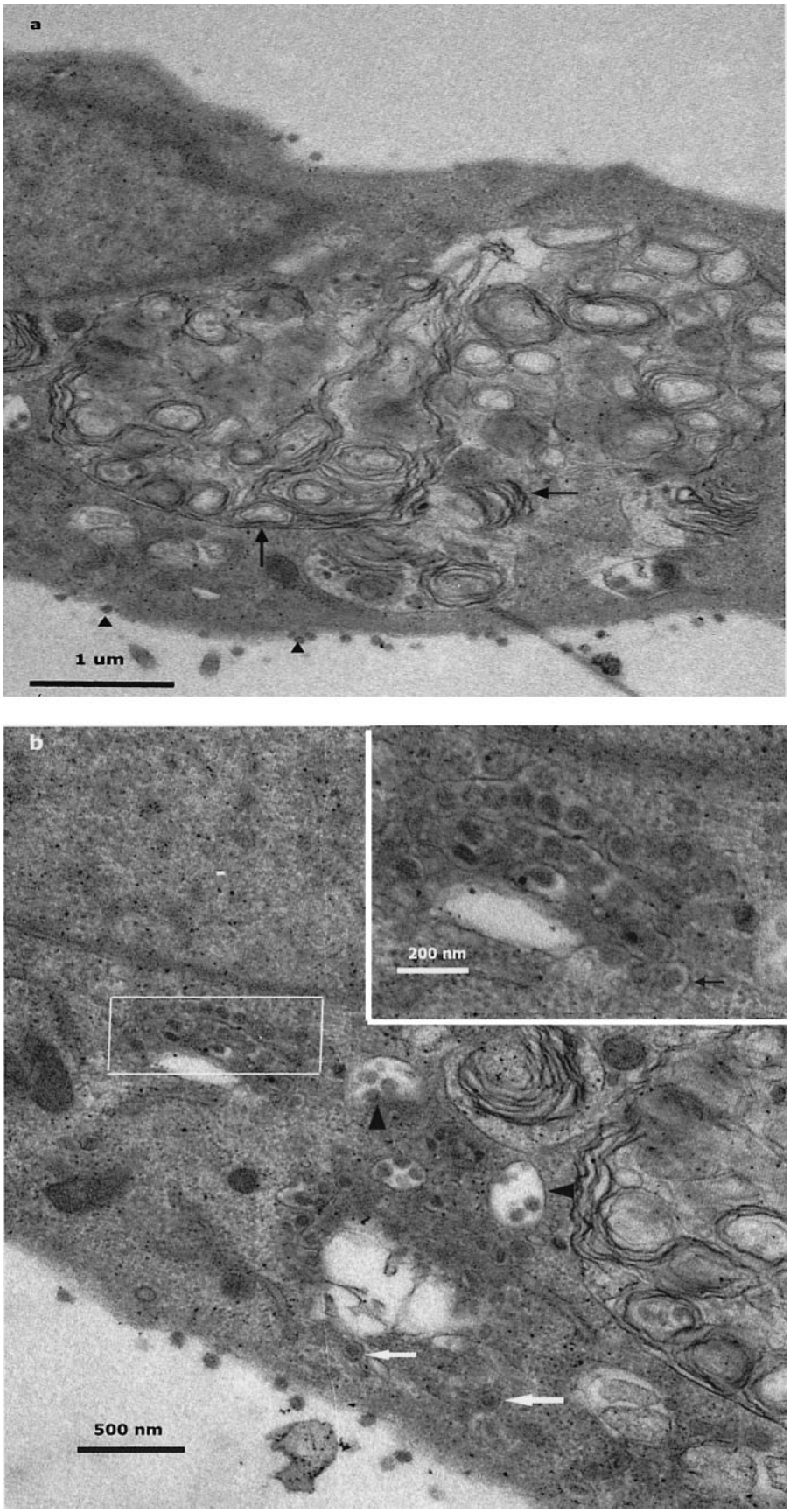

Fig. 3. For legend see page 3296.

Fig. 3. (*on page 3295*) SARS CoV-infected Vero cells at 6 h p.i. (a) Within 6 h of infection, the cell cytoplasm is filled with swollen *trans*-Golgi sacs and most of them are filled with membrane whorls/replication complexes (arrows). Mature virus particles are seen along the outer surface of the plasma membrane (arrowheads). (b) At higher magnification, virus nucleocapsids are seen in the lumen of the Golgi complex (boxed area) as well as in the swollen *trans*-Golgi complex (arrowheads). Inset of the boxed area clearly illustrates virus particles in the process of pinching off the ends of the Golgi sacs (arrow). Single virus particles are also seen moving to the periphery of the cells (white arrows) in small vesicles. Similar to (a), mature virus particles are seen on the outside of the cells.

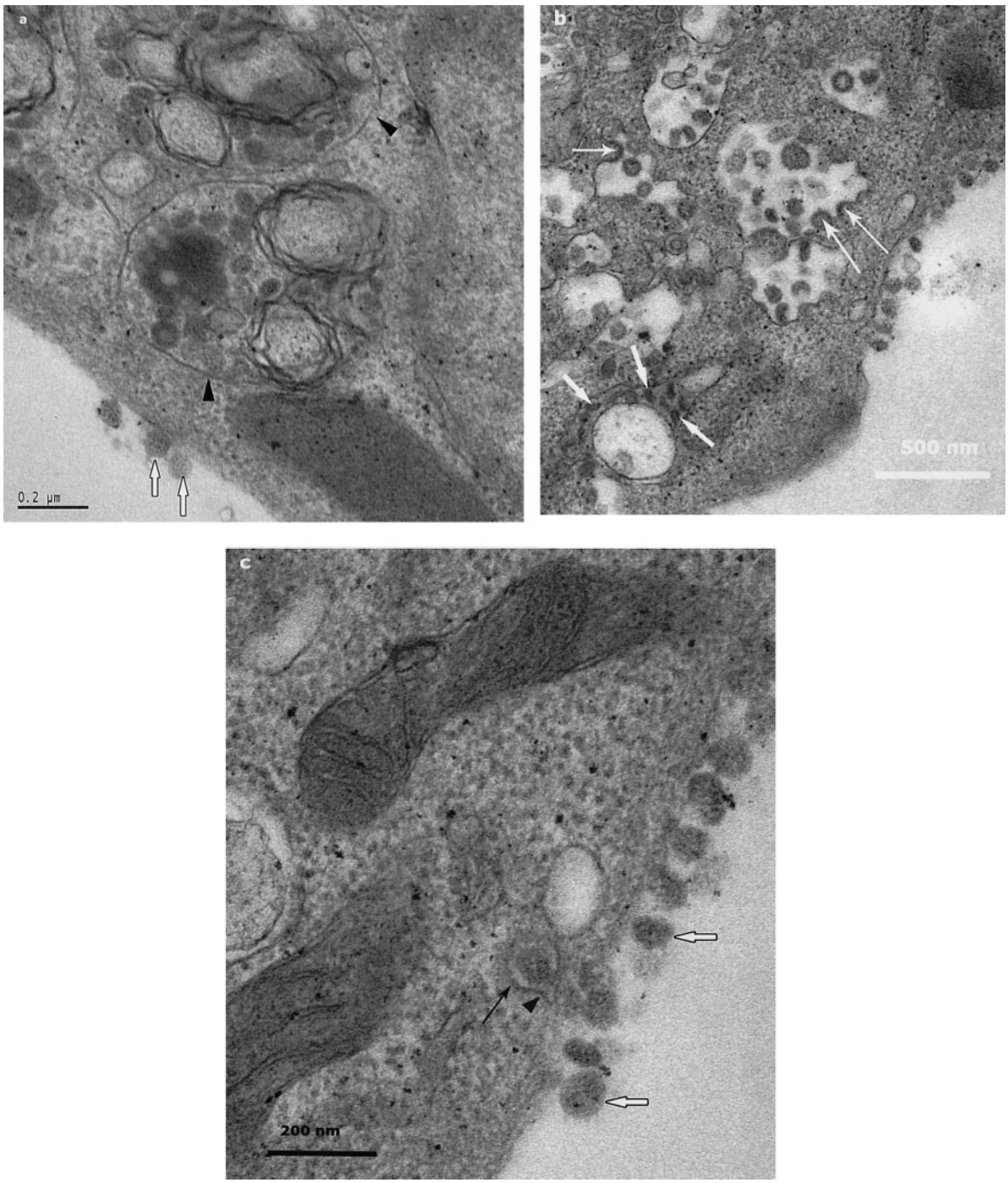

Fig. 4. For legend see page 3299.

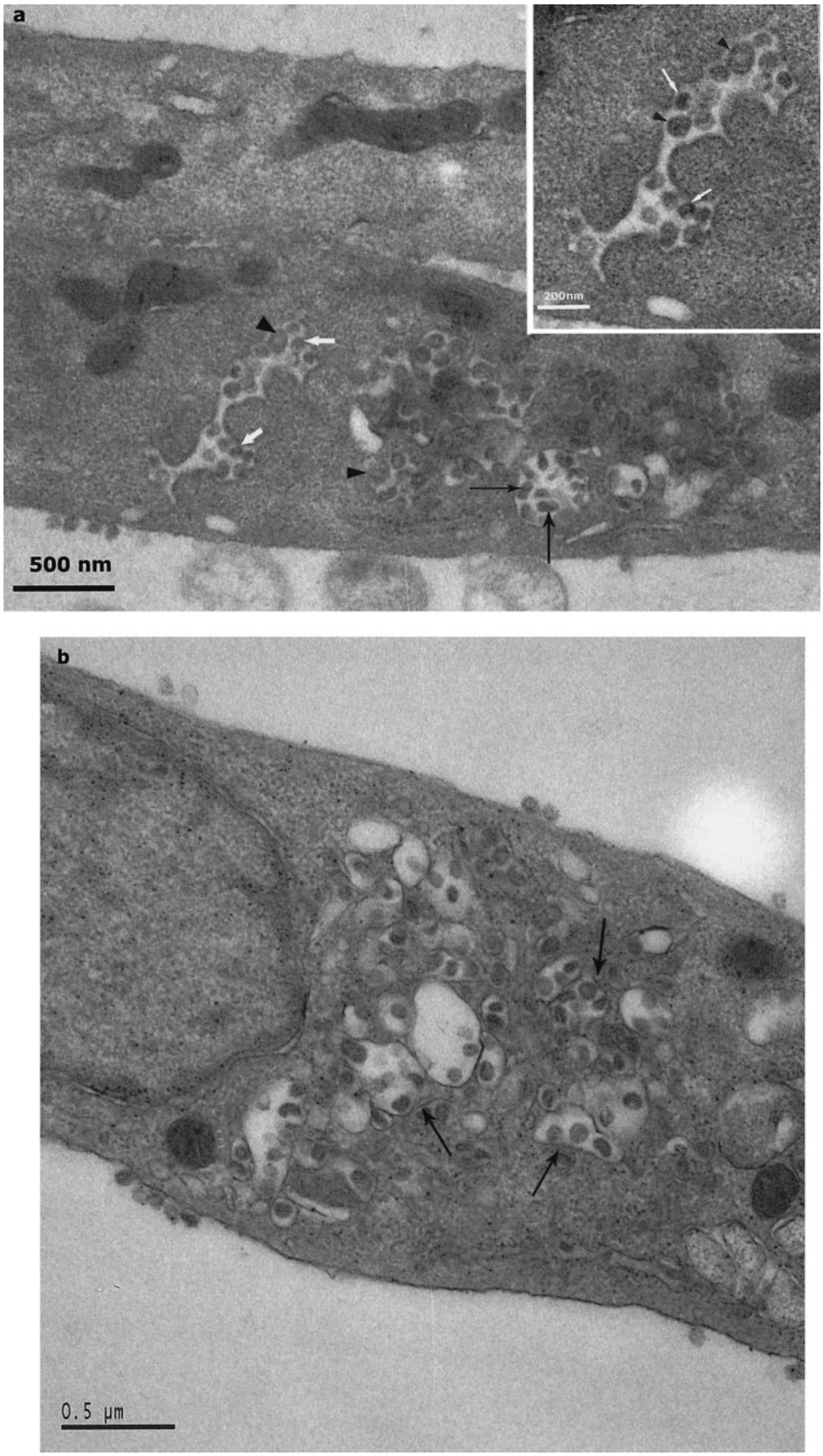

Fig. 5. For legend see page 3299.

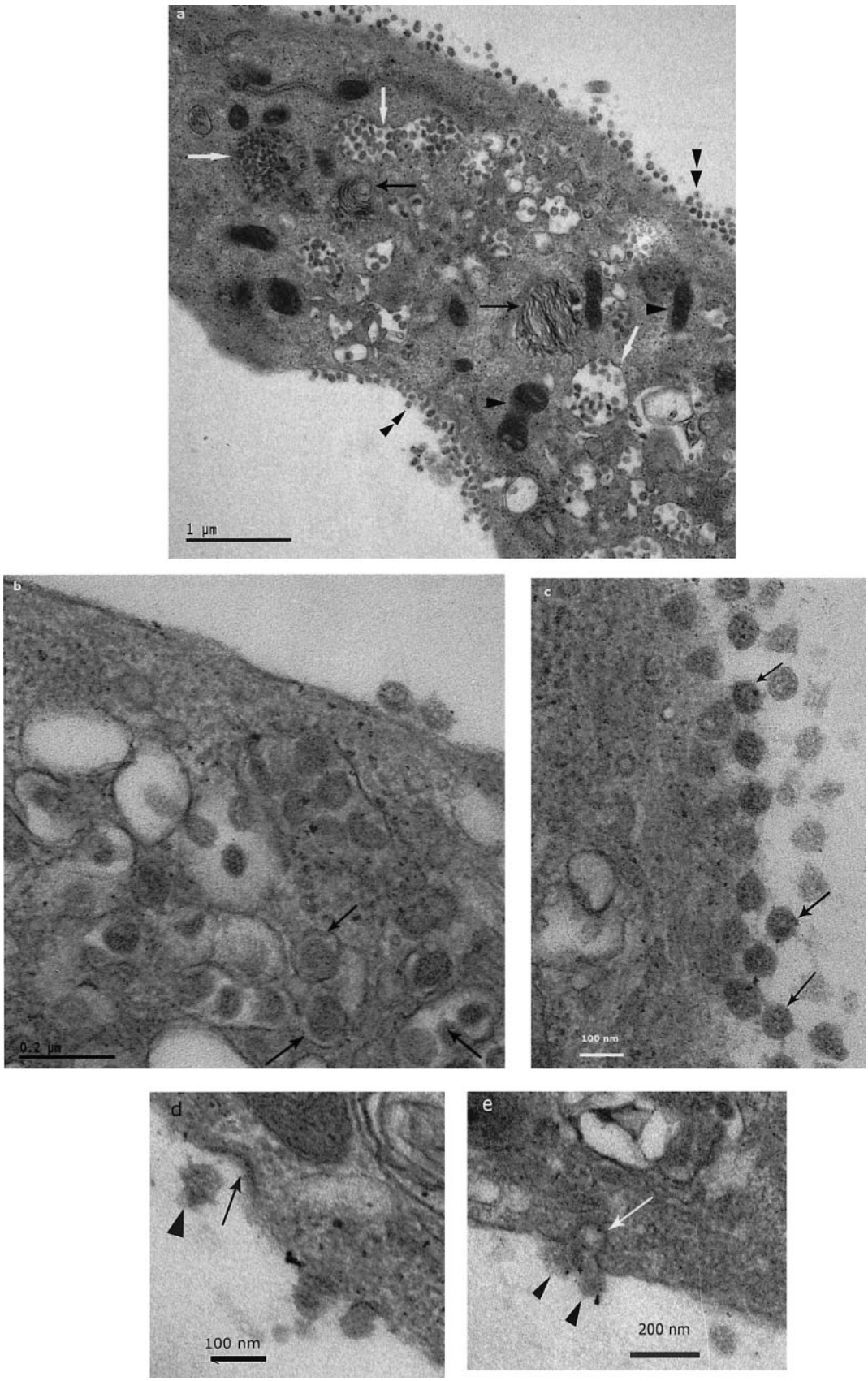

Fig. 6. For legend see page 3299.

Previous studies have reported that coronaviruses assemble by budding into the lumens of the Golgi complex (David-Ferreira & Manaker, 1965; Tooze *et al.*, 1984; Tooze & Tooze, 1985). This mode of assembly was also seen in this study (Fig. 4b). The site of nucleocapsid invagination (Fig. 4b, thin arrows) into the swollen lumens of the Golgi complexes were seen frequently. Doughnut-shaped nucleocapsids were observed to arrange neatly on the cytoplasmic side of the lumen (Fig. 4b, thick arrows) while awaiting budding into the lumen.

In Fig. 4(c), a virus particle within a smaller transport vesicle (arrow) was seen in the process of fusing with the plasma membrane (arrowhead). Many mature virus particles were already exported to the cell surface (Fig. 4c, white arrows).

A low magnification of a typical infected cell at 12 h p.i. is shown in Fig. 5(a). Doughnut-shaped nucleocapsids (Fig. 5a, arrows), spherical cores (white arrows) and mature virus particles (arrowheads) were present in the enlarged vacuoles/swollen Golgi sacs. These different stages of maturation are illustrated more clearly in the inset. Both the 50 nm spherical cores (Fig. 5a, white arrows) and the mature virus particles (80–120 nm) (arrowheads) were present. Besides virus-filled sacs at the periphery of the cells, swollen Golgi sacs at the perinuclear region (Fig. 5b, arrows) were also actively involved in producing progeny virus.

Another striking observation in SARS CoV-infected cells was the intense electron-dense mitochondria (15 h p.i.) (Fig. 6a, arrowheads). These mitochondria appeared to increase in electron density as infection progressed. The significance of this is not known. The usual swollen sacs were filled with membrane layers (Fig. 6a, arrows) and core/mature virus (white arrows). Crystalline arrays of extracellular virus were present all around the infected cells (Fig. 6a, double arrowheads).

By now, more than 50 % of the cell population was actively producing large amounts of virus particles. In Fig. 6(b), mature virus particles (arrows) were observed to pinch off the lumen of the swollen Golgi sacs close to the cell periphery before transportation to cell plasma membrane. The high magnification of the crystalline array of extracellular virus (Fig. 6c) clearly showed the knob-like spikes surrounding the virus particles (arrows).

On some occasions, the extracellular virus particles (arrowheads) were seen to re-enter the infected cells via coated pits (Fig. 6d, e, arrows). At this stage, it is not known if this mode of re-entry into infected cells would yield further productive cycles of replication. Between 15 and 21 h p.i., the percentage of infected cells increased to 70 %. With the longer infection periods, there was a parallel increase in the number of virus-filled vacuoles/swollen Golgi sacs in the infected cytoplasm.

By 24 h p.i., most mature virus particles were seen very close to the plasma membrane awaiting final exit (Fig. 7a). A virus particle (Fig. 7a, arrow) was seen being expelled through a fluke-like channel (arrowhead) created at the plasma membrane. Infected cell filapodia were also active

Fig. 4. (*on page 3296*) SARS CoV-infected Vero cells at 6 h p.i. (a) The membrane whorls/replication complexes are closely associated to maturing virus particles in the large vacuoles (arrowheads). Again, mature virus particles are seen along the extracellular region (white arrows). (b) A more common route of envelopment is the budding of the nucleocapsids into the lumen of the swollen Golgi sacs (thin white arrows). Doughnut-shaped nucleocapsids are also arranged orderly on the cytoplasmic side of these sacs (thick white arrows) awaiting budding into the lumen. (c) Higher magnification electron micrograph of mature virus particles (white arrows) that are commonly visible at just 6 h p.i. A single packaged virus particle in a small vesicle is being transported to the cell surface (arrow). It is believed that the vesicles then fused (arrowhead) to the plasma membrane, extruding the mature virus particles.

Fig. 5. (*on page 3297*) SARS CoV-infected Vero cells at 12 h p.i. (a) This low magnification electron micrograph gives a general view of an infected cell. The cytoplasm is commonly seen filled with bags of doughnut-shaped nucleocapsids (arrows), spherical cores (white arrows) and mature virus particles (arrowheads). The inset gives a clearer view of the spherical cores (50 nm, white arrows) and mature virus particles (80–120 nm, arrowheads). This bag of particles is very close to the cell periphery. (b) At this stage of infection, the Golgi complex sacs are all swollen (arrows) and filled with virus particles at different stages of maturation.

Fig. 6. (*on page 3298*) SARS CoV-infected Vero cells at 12 and 15 h p.i. (a) This cell is a good representation of an infected cell at 15 h p.i. The progressively electron-dense mitochondria (arrowheads) are clearly illustrated. The typical swollen Golgi sacs containing membrane whorls (arrows) and virus particles (white arrows) at different stages of maturation are scattered in the infected cytoplasm. By this stage, numerous extracellular virus particles are seen on both sides of the cell (double arrowheads). (b) Mature virus particles are seen pinching off the swollen Golgi sacs (arrows) into single particle vesicles before transportation to the cell surface. (c) The typical knob-like spikes are clearly visible surrounding most extracellular virus particles (arrows). (d, e) Some virus particles re-attached to the plasma membrane and appear to re-enter the cells via coated pits (arrows). Arrowheads denote virus particles. In (e), two virus particles are vying for one coated pit. The cells infected for 18–21 h p.i. are very similar to those at 15 h p.i. except that there are more virus-filled large vacuoles present in the cytoplasm.

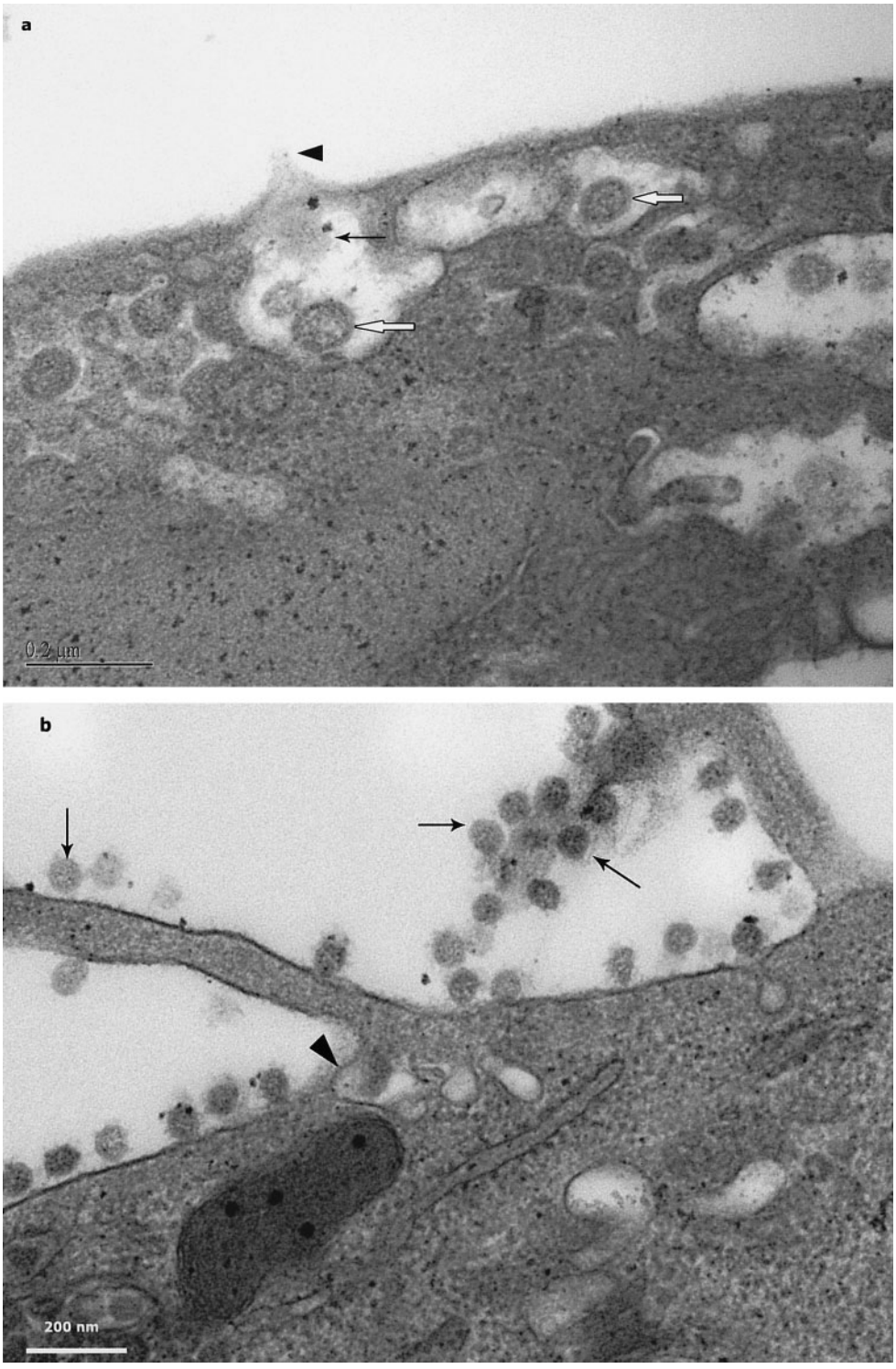

Fig. 7. SARS CoV-infected Vero cells at 24 h p.i. (a) A virus particle (arrow) is in the process of being expelled out onto the cell surface. A channel is created at the plasma membrane (arrowhead). Several mature virus particles (white arrows) are seen near the cell plasma membrane for exportation to the extracellular space. (b) Most of the cells also have mature virus particles lining the cell surface and surface of cell filopodia (arrows). The arrowhead shows a vesicle containing a virus particle just before fusion with the plasma membrane.

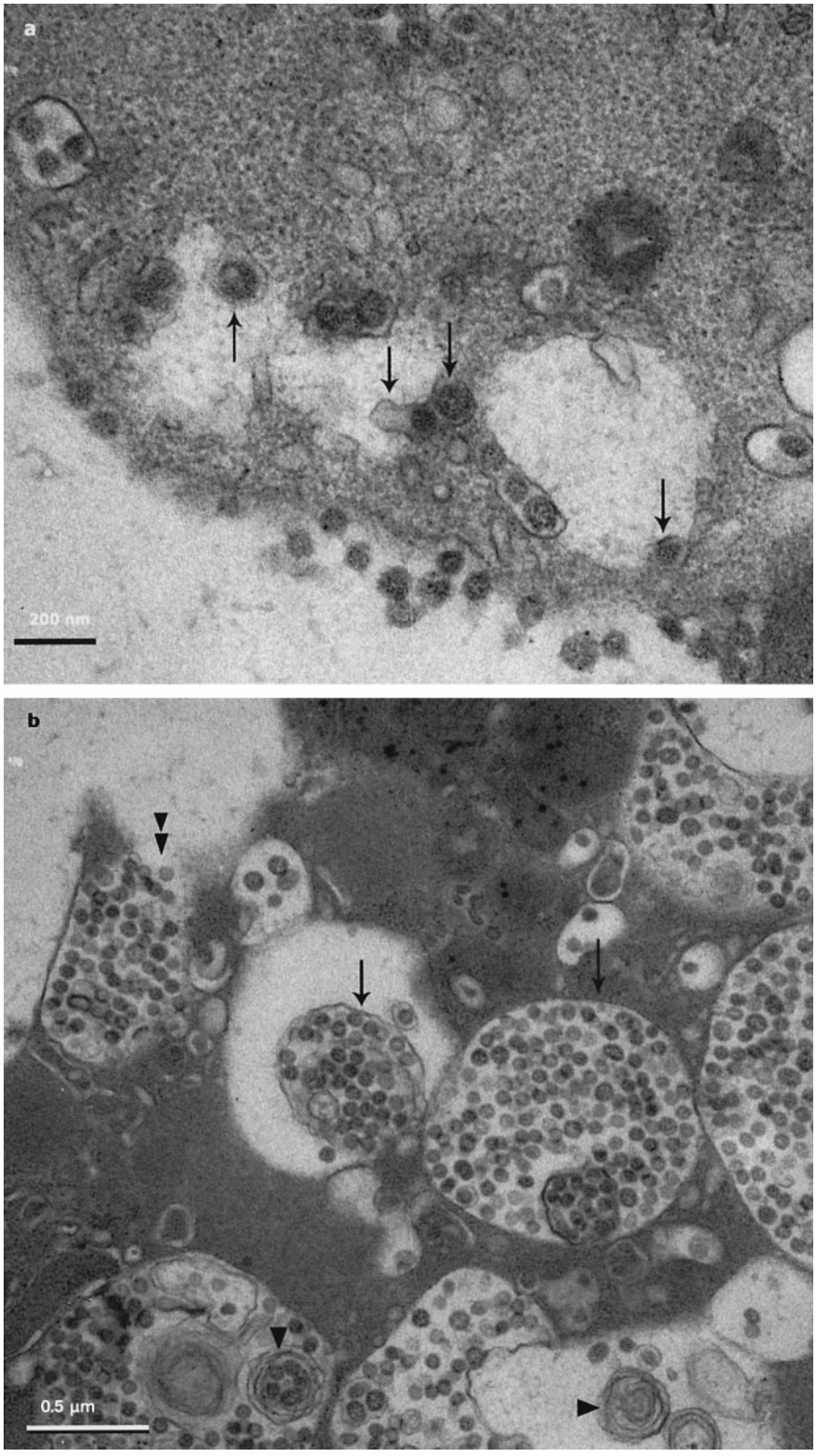

Fig. 8. SARS CoV-infected Vero cells at 30 h p.i. (a) Similar to 24 h p.i., single virus particles pinching off into smaller vesicles (arrows) before exocytosis are seen near the cell periphery. (b) Massive amounts of mature virus particles are found in swollen Golgi sacs (arrows). These sacs now appear as large vacuoles. By this time, most of these large vacuoles contain minimal amounts of the membrane whorls (arrowheads) compared to the earlier times of infection. A large virus-containing vacuole is seen emptying at the breached plasma membrane (double arrowheads).

sites of virus exit (Fig. 7b, arrows). Another virus in the small vesicle was seen just about to fuse with the cell plasma membrane (Fig. 7b, arrowhead).

Single virus particles pinching off from Golgi sacs into small vesicles for their final exit process (Fig. 8a, arrows) were common sights by 30 h p.i. By this stage, almost 100 % of the cells were infected and the cytoplasm of each cell was filled with very swollen sacs consisting mostly of mature virus particles (Fig. 8b, arrows). By now, very few of these sacs contained the membrane whorls (Fig. 8b, arrowheads).

Due probably to the advanced cytopathic effects in these infected cells, the mature virus particles no longer exit in singly packed vesicles. Instead, large bags packed with virus particles fused directly with the plasma membrane (Fig. 8b, double arrowheads). This mode provided fast release of the mature virus particles to the exterior of the dying cells.

DISCUSSION

In this study, SARS CoV was found to replicate extremely well in Vero E6 cells reaching high titres. Despite the fact that it was a human host isolate, it grew well in the monkey kidney cells *in vitro*.

Previous studies have shown that most coronaviruses have a relatively short latent period of 6 h in tissue culture (Sturman & Takemoto, 1972). However, it may take a few days p.i. to achieve high virus yield (Luby *et al.*, 1999). Positive immunofluorescence was obtained 7–14 days p.i. of a human enteric coronavirus in J774 cells (a mouse macrophage cell line). Although the infections could be cytocidal, it was not uncommon to establish persistent infections, as not all cells were infected at the same time (Lucas *et al.*, 1978; Chaloner-Larsson & Johnson-Lussenburg, 1981; Holmes & Behnke, 1981; Lamontagne & Dupuy, 1984).

In this study, SARS CoV was found to have a latent period of only 5 h p.i. By this time, extracellular virus particles were seen (Fig. 2c). In addition, there was evidence of major ultrastructural changes in the infected cell cytoplasm. The Golgi sacs were extensively swollen due to the profuse accumulation of the maturing progeny virus particles within the lumens (Figs 1–4). There was also extensive induction of membrane whorls within the same vacuoles. The membranes evolved very early during infection (within 20–30 min p.i.) (Ng *et al.*, 2003) and could be the replication complexes and site of viral RNA synthesis.

Two types of nucleocapsids were observed during the earlier part of infection (up to 12 h p.i.) (Figs 2, 4a, b and 5). The doughnut-shaped structures probably represented the helical nucleocapsids, which then transformed into the 50 nm spherical core particles before final maturation. These two forms, including mature virus particles of 80–120 nm in diameter, were often found within the same vacuole.

The reported mode of assembly of coronaviruses is by budding into the Golgi lumens (David-Ferreira & Manaker, 1965; Tooze *et al.*, 1984; Tooze & Tooze, 1985). This was also demonstrated in Fig. 4(b, thin white arrows) where nucleocapsids were observed to bud into the swollen lumen of the Golgi complex. Subsequently, the mature virus particles in these large vacuoles were transported to the plasma membrane in pinched off, small, smooth-membraned vesicles (Figs 4c, 6b, 7 and 8a). This supported the previous observation for other coronaviruses (Oshiro, 1973). However, at late times of infection (30 h p.i.), the release of mature virus particles was speeded up by having large bags containing the virus particles fusing directly with the plasma membrane (Fig. 8b). At this stage, 100 % of the cells were infected with SARS CoV and advance cytopathic effects were evident.

From this study, it is concluded that SARS CoV grows faster than other known human coronaviruses, achieving 10^7 p.f.u. ml^{-1} within 24 h p.i. It induces dramatic ultrastructural changes, including the induction of membrane whorls within the same sacs as the virus precursor particles and causes intensive swelling of the Golgi sacs, which become enlarged vacuoles at later stages of infection. Although the ultrastructural changes observed here did not reveal any unique features in the SARS CoV replication cycle compared to other coronaviruses, SARS CoV, nevertheless, replicated quickly *in vitro* after isolation from the human host. Fifty per cent of the cells were infected within 12 h p.i. and this progressed to 100 % by 24 h p.i. There were large accumulations of both intracellular virus particles (in vacuoles) and extracellular virus particles by 12–15 h p.i. The changes in its genomic make-up compared to other known coronaviruses could perhaps enable this new virus to grow equally well both in the human host and in tissue culture (Vero cells).

ACKNOWLEDGEMENTS

Electron microscopy work was performed using a grant from the University Research Grant, National University of Singapore (grant no: 182-000-055-112).

REFERENCES

Chaloner-Larsson, G. & Johnson-Lussenburg, C. M. (1981). Establishment and maintenance of a persistent infection of L123 cells by human coronavirus strain 299E. *Arch Virol* **69**, 117–129.

David-Ferreira, J. F. & Manaker, R. A. (1965). An electron microscope study of the development of a mouse hepatitis virus in tissue culture cells. *J Cell Biol* **24**, 57–78.

Drosten, C., Gunther, S., Preiser, W. & 23 other authors (2003). Identification of a novel coronavirus in patients with severe acute respiratory syndrome. *N Engl J Med* **348**, 1967–1976.

Fleming, J. O., Trousdale, M. D., Stohlman, S. A. & Weiner, L. P. (1987). Pathogenic characteristics of neutralization-resistant variants of JHM coronavirus (MHV-4). *Adv Exp Med Biol* **218**, 333–342.

Fleming, J. O., el-Zaatari, F. A., Gilmore, W., Berne, J. D., Burks, J. S., Stohlman, S. A., Tourtellotte, W. W. & Weiner, L. P. (1988). Antigenic

assessment of coronaviruses isolated from patients with multiple sclerosis. *Arch Neurol* **45**, 629–633.

Frana, M. F., Behnke, J. N., Sturman, L. S. & Holmes, K. V. (1985). Proteolytic cleavage of the E2 glycoprotein of murine coronavirus: host-dependent differences in proteolytic cleavage and cell fusion. *J Virol* **56**, 912–920.

Holmes, K. V. (1990). *Coronaviridae* and their replication. In *Virology*, 2nd edition, pp. 841–856. Edited by B. N. Fields, D. M. Knipe, P. M. Howley, R. M. Chanock, T. P. Monath, J. L. Melnick, B. Roizman & S. E. Straus. New York: Raven Press.

Holmes, K. V. & Behnke, J. N. (1981). Evolution of a coronavirus during persistent infection *in vitro*. *Adv Exp Med Biol* **142**, 287–299.

Holmes, K. V., Doller, E. W. & Behnke, J. N. (1981a). Analysis of the functions of coronavirus glycoproteins by differential inhibition of synthesis with tunicamycin. *Adv Exp Med Biol* **142**, 133–142.

Holmes, K. V., Doller, E. W. & Sturman, L. S. (1981b). Tunicamycin resistant glycosylation of coronavirus glycoprotein: demonstration of a novel type of viral glycoprotein. *Virology* **115**, 334–344.

Holmes, K. V., Frana, M. F., Robbins, S. G. & Sturman, L. S. (1984). Coronavirus maturation. *Adv Exp Med Biol* **173**, 37–52.

Ksiazek, T. G., Erdman, D., Goldsmith, C. S. & 23 other authors (2003). A novel coronavirus associated with severe acute respiratory syndrome. *N Engl J Med* **348**, 1953–1966.

Lamontagne, L. M. & Dupuy, J. M. (1984). Persistent infection with mouse hepatitis virus 3 in mouse lymphoid cell lines. *Infect Immun* **44**, 716–723.

Luby, J. P., Clinton, R. & Kurtz, S. (1999). Adaptation of human enteric coronavirus to growth in cell lines. *J Clin Virol* **12**, 43–51.

Lucas, A., Coulter, M., Anderson, R., Dales, S. & Flintoff, W. (1978). *In vivo* and *in vitro* models of demyelinating diseases. II. Persistence and host-regulated thermosensitivity in cells of neural derivation infected with mouse hepatitis and measles viruses. *Virology* **88**, 325–337.

Marra, M. A., Jones, S. J., Astell, C. R. & 56 other authors (2003). The genome sequence of the SARS-associated coronavirus. *Science* **300**, 1399–1404.

Ng, M.-L., Tan, S.-H., See, E.-E., Ooi, E.-E. & Ling, A.-E. (2003). Entry and early events of severe acute respiratory syndrome coronavirus. *J Med Virol* **71**, 323–331.

Oshiro, L. S. (1973). Coronaviruses. In *Ultrastructure of Animal Viruses and Bacteriophages: an Atlas*, pp. 331–343. Edited by A. J. Dalton & F. Haguenau. Orlando: Academic Press.

Rota, P. A., Oberste, M. S., Monroe, S. S. & 32 other authors (2003). Characterization of a novel coronavirus associated with severe acute respiratory syndrome. *Science* **300**, 1394–1399.

Ruan, Y. J., Wei, C. L., Ling, A.-E. & 17 other authors (2003). Comparative full length genome sequence analysis of 14 SARS coronavirus isolates and common mutations associated with putative origins of infection. *Lancet* **361**, 1779–1785; erratum **361**, 1832.

Sturman, L. S. & Takemoto, K. K. (1972). Enhanced growth of a murine coronavirus in transformed mouse cells. *Infect Immun* **6**, 501–507.

Sturman, L. S. & Holmes, K. V. (1983). The molecular biology of coronaviruses. *Adv Virus Res* **28**, 35–112.

Sturman, L. S., Holmes, K. V. & Behnke, J. (1980). Isolation of coronavirus envelope glycoproteins and interaction with the viral nucleocapsid. *J Virol* **33**, 449–462.

Sussman, M. A., Fleming, J. O., Allen, H. & Stohlman, S. A. (1987). Immune mediated clearance of JHM virus from the central nervous system. *Adv Exp Med Biol* **218**, 399–410.

Tooze, J. & Tooze, S. A. (1985). Infection of AtT20 murine pituitary tumor cells by mouse hepatitis virus strain A59: virus budding is restricted to the Golgi region. *Eur J Cell Biol* **37**, 203–212.

Tooze, J., Tooze, S. A. & Warren, G. (1984). Replication of coronavirus MHV-A59 in sac− cells: determination of the first site of budding of progeny virions. *Eur J Cell Biol* **33**, 281–293.

Wege, H., Siddell, S. & ter Meulen, V. (1982). The biology and pathogenesis of coronaviruses. *Curr Top Microbiol Immunol* **99**, 165–200.

Wilhelmsen, K. C., Leibowitz, J. L., Bond, C. W. & Robb, J. A. (1981). The replication of murine coronaviruses in enucleated cells. *Virology* **110**, 225–230.